

Observation of $S = \frac{1}{2}$ Degrees of Freedom in an $S = 1$ Linear-Chain Heisenberg Antiferromagnet

M. Hagiwara and K. Katsumata

The Institute of Physical and Chemical Research (RIKEN), Wako, Saitama 351-01, Japan

Ian Affleck

Canadian Institute for Advanced Research and Physics Department, University of British Columbia, Vancouver, British Columbia, Canada V6T 2A6

B. I. Halperin

Lyman Laboratory of Physics, Harvard University, Cambridge, Massachusetts 02138

J. P. Renard

Institut d'Electronique Fondamentale, Bâtiment 220, Université Paris-Sud, 91405 Orsay CEDEX, France

(Received 31 July 1990)

The ground state of the typical spin-1 linear-chain Heisenberg antiferromagnet $\text{Ni}(\text{C}_2\text{H}_8\text{N}_2)_2\text{NO}_2(\text{ClO}_4)$ containing a small amount of Cu^{2+} is studied by the electron-spin-resonance (ESR) technique. The ESR results are quantitatively explained by the model that the valence bonds are broken at the Cu^{2+} sites resulting in spin- $\frac{1}{2}$ states at the Ni^{2+} sites neighboring the Cu^{2+} . Thus the present study gives experimental evidence for the existence of the valence-bond-solid ground state in $S=1$ linear-chain Heisenberg antiferromagnets.

PACS numbers: 75.10.Jm, 75.30.Hx, 76.30.Fc

There has been a growing interest in the Haldane-gap problem. According to Haldane's conjecture,¹ the linear-chain Heisenberg antiferromagnet (LCHA) with integer spin values has an energy gap between the nonmagnetic ground state and the first excited one. A number of theoretical²⁻⁷ and experimental⁸⁻¹² works have been published concerning this conjecture. Although there was a controversy about the existence of the Haldane gap, recent theories have proven that the gap does exist. The susceptibility,^{10,11} neutron-scattering,^{10,11} and high-field-magnetization¹² measurements on the spin-1 LCHA compound $\text{Ni}(\text{C}_2\text{H}_8\text{N}_2)_2\text{NO}_2(\text{ClO}_4)$, abbreviated NENP, clearly showed the existence of the Haldane gap in this compound. Despite these efforts, the ground state of the $S=1$ LCHA remains rather difficult to understand intuitively. In $S = \frac{1}{2}$ Heisenberg antiferromagnets, Anderson¹³ has proposed the resonating-valence-bond (RVB) model to describe the ground state. Affleck *et al.*⁶ have extended this idea to the $S=1$ LCHA. They showed that the ground state of an $S=1$ LCHA is well described by the valence-bond-solid (VBS) model. It is shown rigorously⁶ that the correlation function decays exponentially in the VBS state and that an energy gap exists between the ground state and the first excited one. Figure 1(a) shows diagrammatically the $S=1$ VBS state.⁶ Spin 1 is obtained by symmetrization of two $S = \frac{1}{2}$ variables. The spin singlet state can be written with two valence bonds emanating from each site and terminating on different sites.

Let us consider what happens when a host atom is substituted by an impurity atom, for example, Ni^{2+} in NENP by Cu^{2+} . If the exchange interaction between

the host and impurity spins is considerably smaller than that between the host spins, the valence bonds will be broken at the impurity sites. This will result in an $S = \frac{1}{2}$ state at the host spin sites neighboring the impurity [Fig. 1(b)]. For the ordinary Heisenberg Hamiltonian, the effective coupling between these $S = \frac{1}{2}$ degrees of freedom at two ends of a chain is $O((-1)^L e^{-L/\xi} L^{-1/2})$, where L is the chain length and $\xi \approx 7$ is the correlation length. Thus, open chains have low-energy boundary excitations; the Haldane "gap" only exists for bulk excitations. This was demonstrated numerically in Ref. 14. We expect the same behavior for a finite range of anisotropy, presumably in the whole regime of parameters on

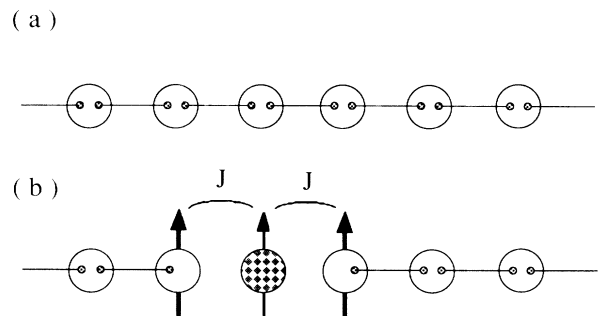


FIG. 1. (a) Diagrammatic representation for the valence-bond-solid ground state of an $S=1$ linear-chain Heisenberg antiferromagnet. The larger circles show the atomic sites and the smaller ones the $S = \frac{1}{2}$ states. The lines represent the valence bonds. (b) A host atom is substituted by an impurity, resulting in spin- $\frac{1}{2}$ states at host sites neighboring the impurity. The arrows show the spin moment.

the boundary of which the bulk gap vanishes.¹⁵ We will be able to get information on the ground state of an $S=1$ LCHA by studying this impurity-induced spin state. Electron spin resonance (ESR) is one of the best methods to study the spin system at a microscopic level. In this paper, we report our ESR study on single crystals of NENP containing a small amount of Cu^{2+} .

First, we summarize the crystal and magnetic properties of NENP. This compound crystallizes in the orthorhombic system.¹⁶ The lattice constants are $a=15.223$ Å, $b=10.300$ Å, and $c=8.295$ Å. The structure consists of a $\text{Ni}(\text{C}_2\text{H}_8\text{N}_2)_2\text{NO}_2$ chain separated by ClO_4 molecules. The magnetic susceptibilities in a single-crystal sample of NENP along the three crystallographic axes show a rounded maximum at about 60 K and decrease abruptly as the temperature is decreased further. The intrachain exchange constant (\mathcal{J}) and the g values along the crystallographic axes (g_a , g_b , and g_c) are determined by fitting the susceptibility data with the theory for an $S=1$ LCHA. The values obtained are¹⁶ $\mathcal{J}=-47.5$ K, $g_a=2.23$, $g_b=2.15$, and $g_c=2.21$. The value of the single-ion anisotropy constant (D) is also estimated from the susceptibility data to be 0.9 K. In the other experiments¹⁰⁻¹² the D value is estimated to be about 10 times larger than this.

The ESR experiment was performed by using standard X-band and K-band spectrometers. The tempera-

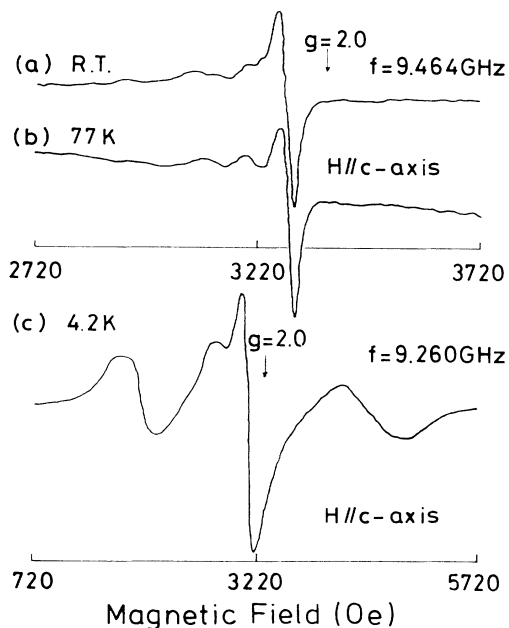


FIG. 2. ESR signals from a single crystal of Cu^{2+} :NENP obtained at (a) room temperature, (b) 77 K, and (c) 4.2 K. These are derivative signals (dI/dH) of the absorption intensity (I) with respect to magnetic field (H). We take for the resonance fields the points at which the dI/dH curves change their sign. Note that the scale of the magnetic field in (c) is expanded compared to (a) and (b).

ture of the sample can be changed from 1.7 K to room temperature. The sample used in this experiment is a single crystal of NENP containing 0.7 at. % Cu^{2+} (nominal concentration). We show in Fig. 2 the ESR signals obtained at room temperature, 77 K, and 4.2 K, respectively, when the external magnetic field is applied along the c axis. The signal at 77 K is almost the same as that at room temperature. On the other hand, the signal at 4.2 K is much different from those at the high temperatures. We have studied the temperature dependence of this signal above 4.2 K. The intensity of the right-most line of Fig. 2(c) is plotted as a function of temperature in Fig. 3. Here, the intensity is defined by $I_{pp}(\Delta H)^2$, where I_{pp} is the distance between the top of the hill and the bottom of the valley of the dI/dH signal along the vertical axis, and ΔH is the corresponding width along the horizontal axis. The intensities of the remaining two lines in Fig. 2(c) behave similarly. We have also investigated the angle dependence of the ESR signals in Cu^{2+} :NENP at $T=4.2$ K. The external magnetic field is rotated in the crystallographic a , b , and c planes. In the a and c planes (the planes containing the chain axis and the direction perpendicular to it), the resonance fields of the left-most and right-most lines in Fig. 2(c) change by about 2500 Oe. On the other hand, in the b plane (the plane perpendicular to the chain axis), the resonance fields change by about 1000 Oe. The resonance field of the central line in Fig. 2(c) does not depend much on the field direction. From these experimental results, it is evident that the ESR lines observed at the low temperatures do not come from free Cu^{2+} ions isolated from the chains. The value of the Haldane-gap energy in NENP has been determined from the

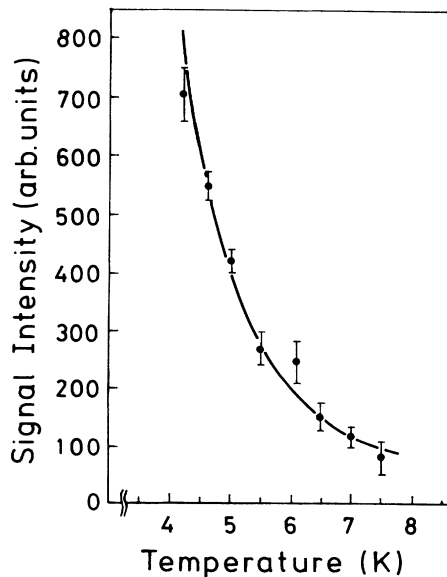


FIG. 3. Temperature dependence of the intensity of the ESR line observed at the low temperatures in Cu^{2+} :NENP.

neutron-scattering study¹⁰ to be 1.17 meV (283 GHz), which is far beyond the frequency of the present experiment. Therefore, one has to look for another origin of the ESR lines.

We calculate the ESR frequencies of the model system presented in Fig. 1(b). The Hamiltonian of the three-spin system when the external magnetic field (H) is directed parallel to the chain axis may be written as

$$\mathcal{H} = -2J_{\parallel}(S_1^z + S_2^z)s^z - 2J_{\perp}\{(S_1^x + S_2^x)s^x + (S_1^y + S_2^y)s^y\} + G_{\parallel}\mu_B H(S_1^z + S_2^z) + g_{\parallel}\mu_B Hs^z, \quad (1)$$

where J_{\parallel} and J_{\perp} are, respectively, the components of the Ni-Cu exchange-interaction constant parallel and perpendicular to the chain axis, S_1 and S_2 ($=\frac{1}{2}$) the spin variables induced at the Ni sites, s ($=\frac{1}{2}$) the Cu^{2+} spin, G_{\parallel} the g value of the spin on the Ni sites along the chain axis, and g_{\parallel} the g value of Cu^{2+} along the chain axis. Note that, despite the much larger D -term anisotropy in the Ni chains, no D term is possible for the effective degrees of freedom at the chain ends because they have $S = \frac{1}{2}$. Therefore, the anisotropy is not larger than the Cu-Ni exchange. Note also that the dipole-dipole interaction between these spins is shown to be small in our case. Since the Cu concentration is small (~ 0.7 at. %), we can neglect the interaction between the Cu^{2+} spins. Taking the Ni-Ni distance along the chain as $\sim 5 \text{ \AA}$,¹⁶ the dipole-dipole interaction is of the order of 0.01 cm^{-1} , which may be neglected compared with the exchange interaction (see below). The Hamiltonian in the case when H is applied perpendicular to the chain axis may be written similarly. Figure 4 shows the eigenvalues of Eq. (1) as functions of H . Here, we have used the following values: $J_{\parallel} = -0.63 \text{ cm}^{-1}$, $J_{\perp} = -0.49 \text{ cm}^{-1}$, $G_{\parallel} = 2.2$, and $g_{\parallel} = 2.2$. The g values are those generally accepted for Ni^{2+} and Cu^{2+} ions. We see that the agreement between the theory and the experiment is good. We have also calculated the intensities of the ESR lines, which agree qualitatively with the experiment. We then compared the theory with the experiment for the external field applied perpendicular to the chain axis. The agreement between the theory and the experiment is also satisfactory in this direction with the same values of J_{\parallel} and J_{\perp} as before and with $G_{\perp} = 2.1$ and $g_{\perp} = 2.1$. We have considered another possibility for the model of the ground state with Cu^{2+} impurity. If we take $S = 1$, instead of $S = \frac{1}{2}$, for the Ni spins neighboring Cu impurities, some of the ESR energies become much higher than those derived from the present model, due to the large D term. We found that the above model could not explain the observed result successfully.

Next, we discuss the temperature dependence of the intensity of the ESR line (Fig. 3). We find that the observed integrated intensity can be fitted, for $4.2 \text{ K} < T < 7.5 \text{ K}$, by the phenomenological formula

$$I = I_0 \{1 - \exp(-\delta/kT)\} \{\exp(E_G/kT) - 1\}, \quad (2)$$

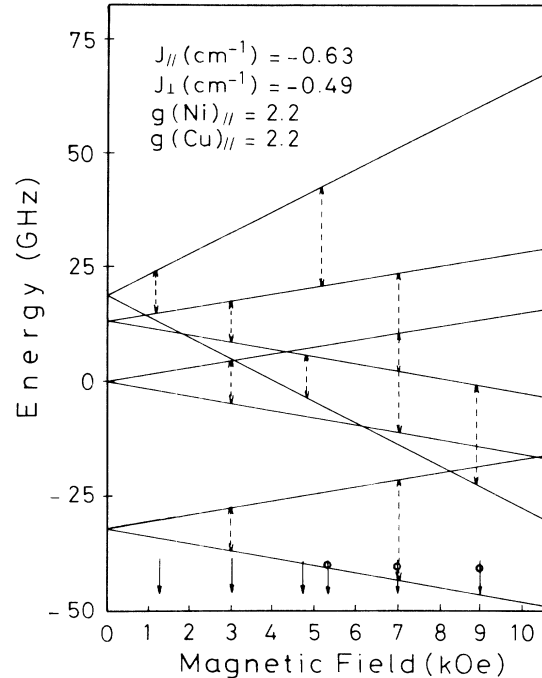


FIG. 4. ESR energy vs external magnetic-field diagram for the model shown in Fig. 1(b). The arrows show the experimental fields obtained at the frequency of 9.25 GHz and the arrows with circles those at 21.7 GHz. The broken arrows represent the theoretical transitions predicted for the frequencies of 9.25 and 21.7 GHz.

the full curve in Fig. 3, where I_0 is a constant. The first factor, where δ is the energy difference between the two levels, is standard, following from the balance between emission and absorption. The second factor, involving the Haldane-gap energy E_G , reflects the growing probability of finding an isolated three-spin system as the temperature is reduced below the Haldane gap. At higher temperatures, magnetic excitations will exist in the bulk of the chains, not just at the ends. These will interact with the three-spin systems, broadening and weakening the ESR signal. The data were fitted by $E_G/k = 13 \text{ K}$, consistent with previous measurements of the Haldane gap in NENP.¹⁰⁻¹²

Finally, we mention the susceptibility of NENP doped with Cu^{2+} . Renard, Regnault, and Verdaguer¹⁷ have measured the susceptibility of Cu^{2+} :NENP. The temperature dependences of the susceptibilities are well fitted by the Curie law at low temperatures with the Curie constants about 4.6 times larger than the calculated ones for free Cu^{2+} impurities. Based on the present model, the Curie constant should be 3 times larger than that for the free- Cu^{2+} case. Further experiments are necessary to clarify this point.¹⁸

In conclusion, we have studied the ground state of the typical $S = 1$ linear-chain Heisenberg antiferromagnet NENP containing a small amount of Cu^{2+} ion by the

ESR technique. The ESR results are quantitatively explained by the model that the valence bonds are broken at the Cu^{2+} sites resulting in spin- $\frac{1}{2}$ states at the Ni^{2+} sites neighboring the Cu^{2+} . This study gives experimental evidence for the existence of the VBS ground state in $S=1$ LCHA.

This work was partially supported by a Grant-in-Aid for Scientific Research from the Japanese Ministry of Education, Science and Culture, by the Natural Sciences and Engineering Research Council of Canada, and by National Science Foundation Grant No. DMR 88-17291. One of us (I.A.) would like to thank Tom Kennedy for useful conversations and for sending a preprint of Ref. 14. Institut d'Electronique Fondamentale is unité associée au CNRS No. 22.

¹F. D. M. Haldane, Phys. Rev. Lett. **50**, 1153 (1983).

²R. Botet and R. Jullien, Phys. Rev. B **27**, 613 (1983).

³R. Botet, R. Jullien, and M. Kolb, Phys. Rev. B **28**, 3914 (1983).

⁴J. B. Parkinson and J. C. Bonner, Phys. Rev. B **32**, 4703 (1985).

⁵M. P. Nightingale and H. W. J. Blöte, Phys. Rev. B **33**, 659 (1986).

⁶I. Affleck, T. Kennedy, E. H. Lieb, and H. Tasaki, Phys. Rev. Lett. **59**, 799 (1987); Commun. Math. Phys. **115**, 477 (1988).

⁷M. Takahashi, Phys. Rev. Lett. **62**, 2313 (1989).

⁸W. J. L. Buyers, R. M. Morra, R. L. Armstrong, M. J. Hogan, P. Gerlach, and K. Hirakawa, Phys. Rev. Lett. **56**, 371 (1986).

⁹M. Steiner, K. Kakurai, J. K. Kjems, D. Petitgrand, and R. Pynn, J. Appl. Phys. **61**, 3953 (1987).

¹⁰J. P. Renard, M. Verdaguer, L. P. Regnault, W. A. C. Erkelens, J. Rossat-Mignod, and W. G. Stirling, Europhys. Lett. **3**, 945 (1987).

¹¹J. P. Renard, M. Verdaguer, L. P. Regnault, W. A. C. Erkelens, J. Rossat-Mignod, J. Ribas, W. G. Stirling, and C. Vettier, J. Appl. Phys. **63**, 3538 (1988).

¹²K. Katsumata, H. Hori, T. Takeuchi, M. Date, A. Yamagishi, and J. P. Renard, Phys. Rev. Lett. **63**, 86 (1989).

¹³P. W. Anderson, Mat. Res. Bull. **8**, 153 (1973).

¹⁴T. Kennedy, J. Phys. Condens. Matter **2**, 5737 (1990).

¹⁵Numerical investigations of this conjecture will be presented elsewhere.

¹⁶A. Meyer, A. Gleizes, J. Girerd, M. Verdaguer, and O. Kahn, Inorg. Chem. **21**, 1729 (1982).

¹⁷J. P. Renard, L. P. Regnault, and M. Verdaguer, J. Phys. (Paris), Colloq. **49**, C8-1425 (1988).

¹⁸From a more detailed analysis, the Curie constant lies between 3.2 and 4.4 depending on the Cu^{2+} concentration and on the field direction; J. P. Renard *et al.* (unpublished).